RSC Advances

ROYAL SOCIETY OF CHEMISTRY

www.rsc.org/advances

Effect of precursor concentration on the properties and tuning of conductivity between p-type and n-type of $Cu_{1-X}Cd_XS_2$ thin films deposited by single step solution process as a novel material for photovoltaic application

V. Nirmal Kumar[1,2], R. Suryakarthick[1], S. Karuppusamy[1], Mukul Gupta[3], Y. Hayakawa[2], R. Gopalakrishnan[1*]

[1]Crystal Research Lab, Department of Physics, Anna University, Chennai, India

[2]Research Institute of Electronics, Graduate School of Science and Technology, Shizuoka University, Hamamatsu, Japan

[3]UGC-DAE Consortium for Scientific Research, Indore, India

Abstract

$Cu_{1-X}Cd_XS_2$ thin films were deposited from precursor solutions having different concentrations of cation sources, by single step solution process at room temperature. The colours of the deposited films changed from light to dark brown based on incorporation of copper and cadmium ions from the precursor. $Cu_{1-X}Cd_XS_2$ polycrystalline thin films exhibit hexagonal structure. Cd rich film showed sheet like morphology and poor adhesiveness owing to cluster growth process. Wider absorption in the region 300 – 1300 nm was observed with red shift in absorption edge as the composition of Cd increased. Relative increase in Cd composition of deposited $Cu_{1-X}Cd_XS_2$ thin films was observed as precursor concentration of Cd increased. XPS and Raman spectra confirmed the formation of $CuCdS_2$ compound. Electrical properties showed the decrease in carrier concentration as Cd composition increases. The $Cu_{1-X}Cd_XS_2$ thin films exhibited both p and n-type conductivity owing to different stoichiometric ratio of cations. The analyses revealed $Cu_{1-X}Cd_XS_2$ thin film can be used as both novel absorber and window layer for the fabrication of low cost thin film solar cells.

Author for correspondence:

*R. Gopalakrishnan

E-mail: krgkrishnan@annauniv.edu, krgkrishanan@yahoo.com

Tel:- 044 – 2235 8710

1. Introduction

Semiconductor materials with significant physical properties have been playing major role for various technological applications. Ternary and quaternary compound/alloy semiconductors, having tuneable physical properties owing to their composition of constituent elements, plays vital role in electronic, optoelectronic, photovoltaic and thermo photovoltaic applications [1]. Metal chalcogenides play promising role for energy conversion and storage devices owing to their unique physical and chemical properties [2]. Apart from III-V compound semiconductors and their alloys, chalcogenide semiconductors based on group VI elements like S and Se, were investigated by many research groups because of ease of synthesis and interesting properties [3,4]. Besides band gap engineering by size reduction in nano materials, alloying them by varying composition of constituent elements results in distinct tuneable properties favourable for wide range of applications [5]. Various ternary and quaternary semiconductor materials were studied for their variation in properties owing to compositional change [6-9]. $CuCdS_2$, a I-II-VI_2 compound is new material in chalcogenide group semiconductor and its physical properties are yet to be revealed. It has tuneable properties between its binary counterparts Cu_xS and CdS. Since copper sulphide exists in five different stable phases at room temperature, it is difficult to differentiate the formation of particular phase Cu_xS [10]. Similarity between the structures of Cu_xS and CdS binary phases was explained in a report by Cook et al, which showed the conversion of CdS single crystal into Cu_xS by dipping it in CuCl solution [11]. Diffusion coefficient of copper in hexagonal-CdS single crystals in perpendicular and parallel direction to c-axis was measured using radio-active tracer technique and reported by Clarke [12]. Moreover, p-type conductivity of CdS doped with copper was enumerated by Kashiwaba et al. and they fabricated solar cell using Cu-doped CdS as absorber layer that recorded 8.5% efficiency [13,14]. Recently, Cu doped CdS nano powders were synthesized by mechanochemical route and their structural and optical properties were reported [15]. So far, a detailed report on $Cu_{1-X}Cd_XS_2$ ternary compound semiconductor is not available yet. The method, which we adapted for the deposition of $Cu_{1-X}Cd_XS_2$ thin film is chemical bath deposition process that is identified as simple, convenient process for large area of deposition and yielding good quality of thin films [16]. As the continuation of our previous work that explains the deposition and properties of $CuCdS_2$ thin films, we now report the

effect of precursor concentration on the deposited $CuCdS_2$ thin films and their variation in physical properties [17].

$Cu_{1-X}Cd_XS_2$ thin films were deposited from precursor solution having various compositions of cation sources by chemical bath deposition method and their physical properties were analysed by X-ray diffraction (XRD), scanning electron microscopy (SEM), electron probe micro analysis (EPMA), X-ray photo electron spectroscopy (XPS), UV-Vis, Raman spectroscopy and Hall effect measurement studies. The suitability of this material as a novel absorber and window layer for the fabrication of thin film solar cells at low cost is analysed.

2. Experiment

2.1 Deposition of $CuCdS_2$ thin films

Thin films of $CuCdS_2$ were prepared with various compositions by chemical bath deposition in single step at room temperature. The schematic of simple chemical bath deposition process is shown in Fig. 1. The precursor solutions for the deposition of $CuCdS_2$ were prepared by dissolving various ratios of $CuSO_4.5H_2O$, $CdSO_4.8H_2O$ and $CS(NH_2)_2$ (thiourea) as cation (Cu^{2+}, Cd^{2+}) and anion (S^{2-}) sources. The concentration of anion is fixed for all reactions and only the cationic concentration (Cu^{2+} and Cd^{2+}) was varied. The concentration of cations and anion sources in precursor solution used for the deposition of $Cu_{1-X}Cd_XS_2$ samples naming A to D, are shown in Table.1. All the samples were prepared simultaneously in different beakers under same conditions at room temperature.

Required amount of $CuSO_4.5H_2O$, $CdSO_4.8H_2O$ and $CS(NH_2)_2$ were dissolved in 100 mL of deionized water and ammonia was added drop by drop until pH of the solution reaches 10.5. While adding ammonia, ultrasonically cleaned glass substrate was immersed vertically in the solution. Addition of ammonia formed complex cation with copper and cadmium ions thereby slow and uniform deposition of the compound made possible owing to slow release of copper and cadmium ions. Compound formation was ensured from the change in colour of the solution from dark/light blue to dark/light brown.

Cu^{2+} and Cd^{2+} ions in the prepared solution from dissolved $CuSO_4$ and $CdSO_4$ were reacted with ammonia to form their complexes tetramine copper ($[Cu(NH_3)_4]^{2+}$) and tetramine cadmium ($[Cd(NH_3)_4]^{2+}$) cations [18,19]. The formation of complex cation from precursor solution is necessary for controlled growth rate. The growth of thin film from a

solution depends on their solubility constant (K_{sp}). As the K_{sp} is low for CdS than Cu_xS, the possibility for the formation of CdS is more when deposited as binary phase. Since the present study involves the deposition of ternary compound ($Cu_{(1-x)}Cd_XS_2$), the process depends on the formation of cations ($[Cu(NH3)4]^{2+}$, $[Cd(NH3)4]^{2+}$) and anion (S^{2-}) and reaction between them.

The reactions involved in the formation of $CuCdS_2$ is as follows [17],

$$CuSO_4 + CdSO_4 + 8NH_3 \rightarrow [Cu(NH_3)_4]^{2+} + [Cd(NH_3)_4]^{2+} + 2SO_4^{2-} \quad (1)$$

Hydrolysis of thiourea took place to release sulphur ions as follows,

$$CS(NH_2)_2 + OH^- \rightarrow CH_2N_2 + H_2O + HS^- \quad (2)$$

$$HS^- + OH^- \rightarrow S^{2-} + H_2O \quad (3)$$

($[Cu(NH_3)_4]^{2+}$, $[Cd(NH_3)_4]^{2+}$) and anions (S^{2-}) reacted and formed the ternary compound $CuCdS_2$ in the solution as follows,

$$[Cu(NH_3)_4]^{2+} + [Cd(NH_3)_4]^{2+} + 2S^{2-} \rightarrow CuCdS_2 + 8NH_3 \quad (4)$$

The heterogeneous nucleation occurs along with homogeneous nucleation in the solution and $Cu_{1-X}Cd_XS_2$ thin films were formed on glass substrate. After 40 minutes the deposited films were taken out, rinsed and cleaned ultrasonically to remove loosely adhered particles. Under ultrasonification samples A, B and C were not peeled from substrate which revealed well adhesiveness of $Cu_{1-X}Cd_XS_2$ thin films whereas sample D was peeled after some time from substrate that showed comparatively poor adhesiveness. The $Cu_{1-X}Cd_XS_2$ films were dried in oven at 50˚C and subjected for further characterization.

2.2 Characterization of $CuCdS_2$ thin films

The deposited $CuCdS_2$ films were subjected to XRD, SEM, EPMA, XPS, UV-Vis, Raman and Hall effect measurement studies to analyse their physical properties. XRD pattern of the deposited thin films was recorded with CuKα radiation by Bruker D8 advance XRD system. Elemental analysis and surface morphology studies were performed by JEOL-JXA 8530F field emission electron probe micro analyser. Optical absorbance in the range 300 – 1300 nm was recorded by Perkin Elmer Lambda 950 system with uncoated glass slides as reference. Raman spectra of the deposited thin films in the range 100 - 1600 cm^{-1}

were recorded by Jobin Yvon Horibra LABRAM-HR visble system. Ar ion laser having excitation wavelength 488 nm, with spot size 1 μm, was used for recording the Raman spectrum. The spectra were recorded at room temperature by CCD camera having 600 lines/mm gratings with spectral resolution of about 1 cm^{-1}. Hall effect measurement was made using Ecopia Hall effect measurement system (HMS – 3000) to analyse the electrical properties of the deposited thin films.

3. Results and Discussion

3.1 Structural properties

The recorded XRD pattern of deposited thin film as shown in Fig,2 was indexed using Crysfire software. All the deposited films exhibit poly crystalline nature with hexagonal structure. Among the four thin films, sample B (3:2) and sample C (2:3) were consist of nearly equal composition of Cu^{2+} and Cd^{2+} ions that showed nearly similar pattern in XRD. They commonly have the primary peak at 2θ value 31.9˚, that corresponds to (103) plane. Samples A (Cu rich) and D (Cd rich) have primary peaks at 38.3˚ and 31.7˚, owing to respective (103) and (102) planes. The observed shift in the primary peaks of each sample was due to the change in lattice parameter values. The lattice parameters of $Cu_{(1-X)}Cd_XS_2$ thin films having different compositions were calculated. The change in lattice parameter value upon varying the cation composition is shown in table.2. From the table it has been found that the unit cell volume and c/a ratio both were increased upon increasing the Cd composition. These results had shown that the composition variation in deposited thin films significantly varied the structural parameters of $Cu_{1-X}Cd_XS_2$ compound. All the four $Cu_{1-X}Cd_XS_2$ thin films had hexagonal structure which was in consistent with our earlier work on analysis of $CuCdS_2$ thin film [17].

3.2 Morphological and elemental analysis

Surface morphologies of $CuCdS_2$ thin films analysed by SEM are shown in Figs. 3(a)-(d) that revealed the formation of continuous, pin hole free coating of deposited material and particles aggregation were changed from spherical to sheet like morphology upon increasing cadmium content in the deposited films. The solubility constant (K_{sp}) is greater for Cu_xS (35.1) than CdS (15.9). Since the solubility constant is low for CdS, aggregations of particles were formed as Cd composition increased. The sheet like morphology in Cd rich film revealed the cluster growth process that resulted in poor adhesiveness of sample D, whereas

ion-by-ion process revealed by SEM micrographs of samples A, B and C resulted in better adhesiveness of samples with substrate. The thicknesses of $Cu_{(1-X)}Cd_XS_2$ thin films were measured by taking cross-sectional SEM images which were shown as inset in fig. 3. The thicknesses of thin film were in the range 8.5 to 38 μm.

Compositions of deposited material measured by EPMA are shown in Table. 3. It showed that the composition of cadmium increases from samples A to D owing to relative precursor concentrations. Cd and S compositions in deposited $CuCdS_2$ thin films were calculated and plotted as shown in Fig. 4. It revealed that the sulphur composition was almost same and the cation composition only varied in all deposited $CuCdS_2$ thin film

XPS spectra of $CuCdS_2$ thin films showing Cu 2p, Cd 3d and S 2p levels are presented in Figs. 5 (a), (b), and (c) and the obtained binding energy values are given in Table. 4. It is inferred from the table that the binding energy values have shift from reported binary phases CuS, Cu_2S and CdS [20,21]. The shift in binding energies between binary and ternary phases resulted from interaction between cations of different groups (Cu and Cd). Increase in binding energy of Cu 2p level ranging between 933.9 – 935.6 eV was observed as the composition of Cu decreases from sample A to D. The binding energy initially decreased from 409.31 to 407.02 eV in Cd 3d level and increased gradually as the composition of cadmium increases from sample B to D. The decrease in intensity of Cd 3d and Cu 2p levels was observed in Cu rich (sample A) and Cd rich (sample D) thin films. Even though the concentration of sulphur source in all reactions and sulphur composition was almost same in deposited thin films, binding energy of S 2p increases from 162.6 to 164 eV in samples A-D. The band structure of CdS is altered by Cu ions by the formation of space charge region (band bending). Since Cu ions act as acceptor centre, higher concentration of Cu ion in CdS altered its conductivity from n-type to p-type that resulted in p-type conductivity of Cu rich sample (Sample A) in our present study.

The shift in binding energies of Cu 2p and Cd 3d levels were attributed to band bending of both CdS and Cu_xS binary phases. However the band bending of Cu_xS is more when compared to CdS. Moreover the band alignment of Cu_2S/CdS system showed that the conduction band minimum of both systems is nearly equal. Hence the energy loss due to charge transport from Cu_2S to CdS is much less and this system is suitable for charge injection and carrier transport [22].

3.3 Optical properties

3.3.1 UV-Vis spectral analysis

The optical response of deposited materials were recorded and absorption coefficient was calculated using the formula a = 2.303 A/t, where t is the film thickness. The calculated absorption co-efficient was plotted as a function of wavelength and it was shown in **Fig 6 (a)** that revealed the material has wide range of absorption in 300 – 1300 nm region which is favourable for photovoltaic applications since maximum number of photons in solar spectrum approaching earth having wavelength in visible and near-IR regions. From the plot it was observed the absorption coefficient decreased as the Cd composition increased. A blue shift of absorption edge was observed in the spectra as the composition of Cd increased. The composition change caused the change in band gap in the range 1.46 to 1.85 eV. Band gap of deposited material was found using Tauc's plot as shown in Fig. 6 (b), which were increased, ranging 1.46 – 1.85 eV as the composition of cadmium increases.

A thin film solar cell is made of p and n type semiconductor materials are kept in contact. The band gap of those materials play key role in energy conversion. Under illumination of light, the charge carriers of p-type absorber layer can absorb photons of energy equal or higher to its band gap. On the other hand, the n-type semiconductor material should have higher band gap than absorber layer so that it can transmit photons of energy below its band gap. Hence the p and n- type semiconductors should have optimum band gap so as to utilize more number of photons in solar spectrum. The optimum band gap for the potential utilization of solar spectrum is between 1-1.5 eV as maximum number of photons in sunlight approaching earth atmosphere lies in the range. Moreover the band gap of p and n-type layers should not have much variation between them. The voltage developed during absorption process should be high enough to drive charge carriers before recombination occurs. Considering these factors, the difference between band gap energies of p and n- type layers should be less than 1 eV. In our present study, the band gap of Cu rich $Cu_{(1-X)}Cd_XS_2$ (sample A) is 1.46 eV and Cd rich $Cu_{(1-X)}Cd_XS_2$ (sample D) is 1.85 eV. The variation between them is 0.39 eV. By considering the above said factors the deposited $Cu_{(1-X)}Cd_XS_2$ can potentially be utilized for the fabrication of solar cells.

The variation in band gap of $Cu_{1-X}Cd_XS_2$ thin films is plotted as a function of Cd composition as shown in Fig 7. The increase in band gap is observed from the graph as the composition of Cd increased, whereas decrease in band gap was observed with Cu rich,

ternary and quaternary compounds owing to p-d hybridization between Cu-d levels and Se p-levels, but in the present case S p-levels [23,24].

3.3.2 Raman Analysis

The vibration modes of binding state existing between Cu, Cd and S atoms were recorded by Raman spectrum (Fig. 8). Three peaks were observed at 298.9, 473.3 and 601.8 cm^{-1}. The peaks at 298.9 and 601.8 cm^{-1} were attributed to 1LO and 2LO processes of CdS which nearly match with reported values. The peak at 473.3 cm^{-1} was resulted from S-S stretching mode of A1g symmetry assigned to CuS [25]. However, shift was observed in Raman peaks for Cu_xS (472 and 474 cm^{-1}) and CdS (305, 600 and 904 cm^{-1}) binary phases [26,27]. The large shift in Raman peaks may be attributed to stress developed in the material [28]. The stress developed in the deposited $CuCdS_2$ thin films is due to lattice strain between Cu_xS and CdS binary phases formed during the deposition process.

3.4 Electrical properties

Electrical properties of deposited $Cu_{1-X}Cd_XS_2$ thin films were studied by Hall effect measurement system and the data obtained are shown in Table 4. From the data it is observed that the carrier concentration decreases as Cd composition increases (sample A to D). Cu rich films (sample A) have shown higher carrier concentration with lower resistivity and higher mobility. The conductivity changed from p-type to n-type as the composition of Cd increases. Sample A showed p-type conductivity whereas, the other samples B, C and D showed n-type conductivity. The concentrations of sulphur source in precursor solution and anion composition in deposited $Cu_{1-X}Cd_XS_2$ thin films were found to be same for all the compositions. Hence the variation in stoichiometry of Cu and Cd determines the type of carriers which is in agreement with earlier report [29]. A high concentration of p-type carriers in heavily Cu doped CdS is observed owing to copper 3d levels. [30]. P-type conductivity in Cu rich film was resulted from Cu ions acts as acceptor centers [31]. $Cu_{1-X}Cd_XS_2$ thin films exhibit both p-type and n-type conductivity owing to stoichiometry of cation compositions.

The p-type $Cu_{(1-X)}Cd_XS_2$ (sample A) has higher carrier concentration of the order of 10^{18} and has lower resistivity. During absorption process the generated charge carries at the pn-junction can transport through absorber that has lower resistivity driven by developed high potential in pn-junction as the difference between the band gap is as low as 0.39 eV.

Though the n-type $Cu_{(1-X)}Cd_XS_2$ (sample D) shown one order of higher magnitude in resistivity than p-type $Cu_{(1-X)}Cd_XS_2$ (sample A), its mobility is high enough to transport charge carriers though it. The optimum band gap and suitable electrical properties of $Cu_{(1-X)}Cd_XS_2$ thin films can be helpful for making efficient photovoltaic device.

4. Conclusion

$Cu_{1-X}Cd_XS_2$ thin films with different compositions were deposited on glass substrates from precursor solution that had various concentrations of cation and anion sources. XRD analysis revealed the hexagonal structure of deposited films and change of lattice parameters upon varying the composition. SEM image showed continuous coating of thin films with morphology changed from spherical to sheet like structure owing to cluster growth process of Cd rich films. EPMA measurement showed the composition of S remains same and cation compositions change. Relative variations in the Cd composition of deposited films were observed as the precursor concentration varies. Increase in binding energies of Cu 2p, Cd 3d and S 2p levels were observed as the composition of cadmium increases owing to shift in valance band structure from Cu_xS to CdS. The deposited material has wider absorption in 300 – 1300 nm range and there is red shift in absorption edge as the Cd composition increased. Band gap of $Cu_{1-X}Cd_XS_2$ thin film increases from 1.46 eV to 1.85 eV for Cu to Cd rich composition. Raman peaks were observed at 298.9, 601.8 and 473.3 cm^{-1} owing to vibration modes of its binary phases CdS and Cu_xS, respectively. Carrier concentration of $CuCdS_2$ thin films decreases as the composition of Cd increased in deposited thin films. The same material, $CuCdS_2$ thin films exhibited two different type conductivities, p and n-type owing to composition of cations. Cu rich film showed p-type conductivity, whereas Cd rich samples showed n-type conductivity. Physical properties of $Cu_{1-X}Cd_XS_2$ thin films can be tuned between Cu_xS and CdS to get desired properties. Since $Cu_{1-X}Cd_XS_2$ thin films with Cu and Cd rich compositions had wider absorption region, p and n-type conductivities, higher carrier concentration and tuneable band gap between Cu_2S and CdS, this material is suitable for photovoltaic applications and the same material ($Cu_{1-X}Cd_XS_2$) can perform the role of both p-type and n-type semiconductor based on their composition.

References

[1] S. Adachi, Properties of semiconductor alloys: Group IV, III-V, II-VI Semiconductors, Wiley, (2009) 1-400.

[2] M. R. Gao, Y. F. Xu, J. Jiang, S. H. Yu, Chem. Soc. Rev. 42 (2013) 2986.

[3] X. Liu, Z. Liu, F. Meng, M. Sugiyama, Solar Energy Materials & Solar Cells 124 (2014) 227–231

[4] P. Chen, M. Qin, H. Chen, C. Yang, Y. Wang, F. Huang, Phys. Status Solidi A 210-6, (2013) 1098.

[5] M. D. Regulacio, M. Y. Han, Accounts of Chemical Research, 43 (2010) 621.

[6] F. D. Benedetto, I. Bencista, S. Caporali, S. Cinotti, A. D. Luca, A. Lavacchi, F. Vizza, M. M. Miranda, M. L. Foresti, M. Innocenti, Prog. Photovolt: Res. Appl. 22 (2014) 97.

[7] S. Theodoropoulou, D. Papadimitriou, K. Anestou, C. Cobet, N. Esser, Semicond. Sci. Technol. 24 (2009) 015014.

[8] Z. Aissa, M. Amlouk, T. Ben Nasrallah, J.C. Bernede, S. Belgacem, Solar Energy Materials & Solar Cells 91 (2007) 489.

[9] D. B. Khadka, J. H. Kim, J. Phys. Chem. C, 118 (2014) 14227.

[10] S.Y. Wang, W. Wang, Z. H. Lu, Materials Science and Engineering B103 (2003) 184.

[11] W. R. Cook, L. Shiozawa, F. Augustine, J. Appl. Phys., 41 (1970) 3058.

[12] R. L. Clarke, J. Appl. Phys., 30 (1959) 957.

[13] Y. Kashiwaba, I. Kanno, T. Ikeda, Jpn. J. Appl. Phys., 31 (1992) 1170.

[14] Y. Kashiwaba, K. Isojima, K. Ohta, Solar Energy Materials & Solar Cells, 75 (2003) 253.

[15] P. Reyes, S. Velumani, Materials Science and Engineering B 177 (2012) 1452.

[16] R. S. Mane, C. D. Lokhande, Materials Chemistry and Physics, 65 (2000) 1.

[17] V. Nirmal Kumar, R. Suriakarthick, Y. Hayakawa, S. Hussain, G.M. Bhalerao, M. Gupta, V. Sathe, R. Gopalakrishnan, Superlattices and Microstructures, 76 (2014) 125.

[18] M. T. S. Nair, P. K. Nair, Semicond. Sci. Technol. 4 (1989) 191.

[19] N. R. Pavaskar, C. A. Menezes, A.P.B. Sinha, J. Electrochem. Soc. 124 (1977) 743.

[20] Y. B. He, A. Polity, I. Osterreicher, D. Pfisterer, R. Gregor, B. K. Meyer, M. Hardt, Physica B, 308–310 (2001) 1069.

[21] D. M. Poirier, J. H. Weaver, Surface Science Spectra, 2 (1993) 249.

[22] G. Liu, T. Schulmeyer, J. Brotz, A. Klein, W. Jaegermann, Thin Solid Films 431 – 432 (2003) 477.

[23] R. Noufi, R. Axton, C. Herrington, S. K. Deb, Appl. Phys. Lett., 45 (1984) 668.

[24] G. Suresh Babu, Y. B. Kishore Kumar, P. Uday Bhaskar, S. Vanjari, Solar Energy Materials & Solar Cells, 94 (2010) 221.

[25] M. Ishii, K. Shibata, H. Nozaki, Journal of Solid State Chemistry, 105 (1993) 504.

[26] D. S. Chuu, C. M. Dai, W. F. Hsieh, C. T. Tsai, J. Appl. Phys., 69 (1991) 8402.

[27] L. A. Isac, A. Duta, A. Kriza, I. A. Enesca, M. Nanu, Journal of Physics: Conference Series 61 (2007) 477.

[28] R. J. Briggs, A. K. Ramdas, Physical Review B, 13 (1976) 5518.

[29] R. Noufi, R. Axton, C. Herrington, S. K. Deb, Appl. Phys. Lett., 45 (1984) 668.

[30] E. D. Fabricius, J. Appl. Phys., 33 (1962) 1597.

[31] F. Arjona, E. Elizalde, E. G. Camarero, A. Feu, B. Lacal, M. Leon, J. Llabres, F. Rueda, Solar Energy Materials 1 (1979) 379.

S. No.	Sample	Concentration (M/L)			Solution Volume (mL)
		$CuSO_4.5H_2O$	$CdSO_4.8H_2O$	$CS(NH_2)_2$	
1.	A	0.08	0.02	0.2	100
2.	B	0.06	0.04	0.2	
3.	C	0.04	0.06	0.2	
4.	D	0.02	0.08	0.2	

Table 1: Precursor concentrations of cations and anions for the deposition of $Cu_{1-X}Cd_XS_2$ thin films

Sample	Lattice Parameter (Å)		c/a ratio	Unit cell volume ($Å^3$)
	a	c		
A	3.247	12.944	3.86	117.125
B	3.522	13.606	4.05	146.182
C	3.281	13.317	4.13	124.192
D	3.529	14.584	3.86	157.329

Table 2: Observed lattice parameters of $Cu_{1-X}Cd_XS_2$ thin films

S. No.	Sample	Elemental compositions in $CuCdS_2$ thin films			Cd Composition [Cd/(Cu+Cd)] (%)
		Cu	Cd	S	
1	A	62.90	0.34	36.76	0.5
2	B	55.07	11.80	33.13	17.7
3	C	48.38	17.56	34.06	26.6
4	D	7.53	63.38	29.09	89.4

Table 3: Composition of $Cu_{1-X}Cd_XS_2$ thin films measured by EPMA

S. No	Sample	Binding energies (eV)				
		Cu 2p		Cd 3d		S 2p
		3/2	1/2	5/2	3/2	
1.	A	933.9	953.7	409.31	-	162.6
2.	B	934.6	954.5	407.02	413.91	163.3
3.	C	934.7	954.5	407.23	414.01	163.5
4.	D	935.6	954.7	407.28	414.07	164

Table 4: Binding energies of Cu2p, Cd 3d and S 2p levels of $Cu_{1-X}Cd_XS_2$ thin films measured by XPS

S. No.	Sample	Carrier Concentration (cm-3)	Resistivity (Ωcm)	Mobility (cm^2/Vs)	Type of charge carriers
1	A	3.48×10^{18}	0.16	10.6	p-type
2	B	1.57×10^{14}	2.41×10^{4}	1.64	n-type
3	C	4.07×10^{13}	5.66×10^{4}	2.7	n-type
4	D	1.8×10^{12}	3.5×10^{5}	15.06	n-type

Table 5: Electrical properties of deposited $Cu_{1-X}Cd_XS_2$ thin films

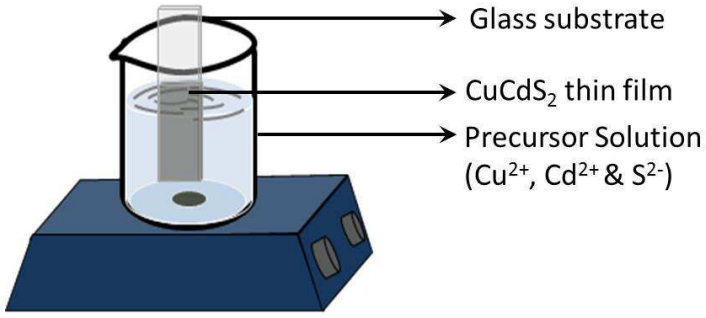

Fig. 1. Schematic of simple chemical bath deposition process

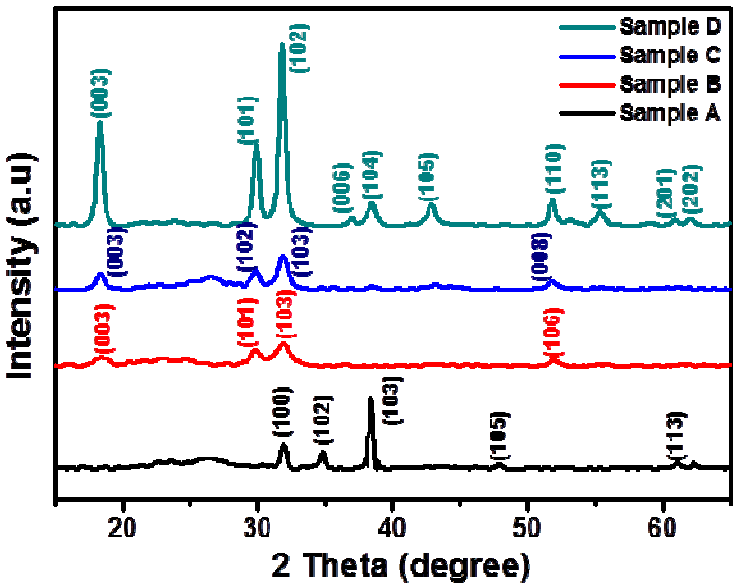

Fig. 2. XRD patterns of $Cu_{1-X}Cd_XS_2$ thin film samples A, B, C and D

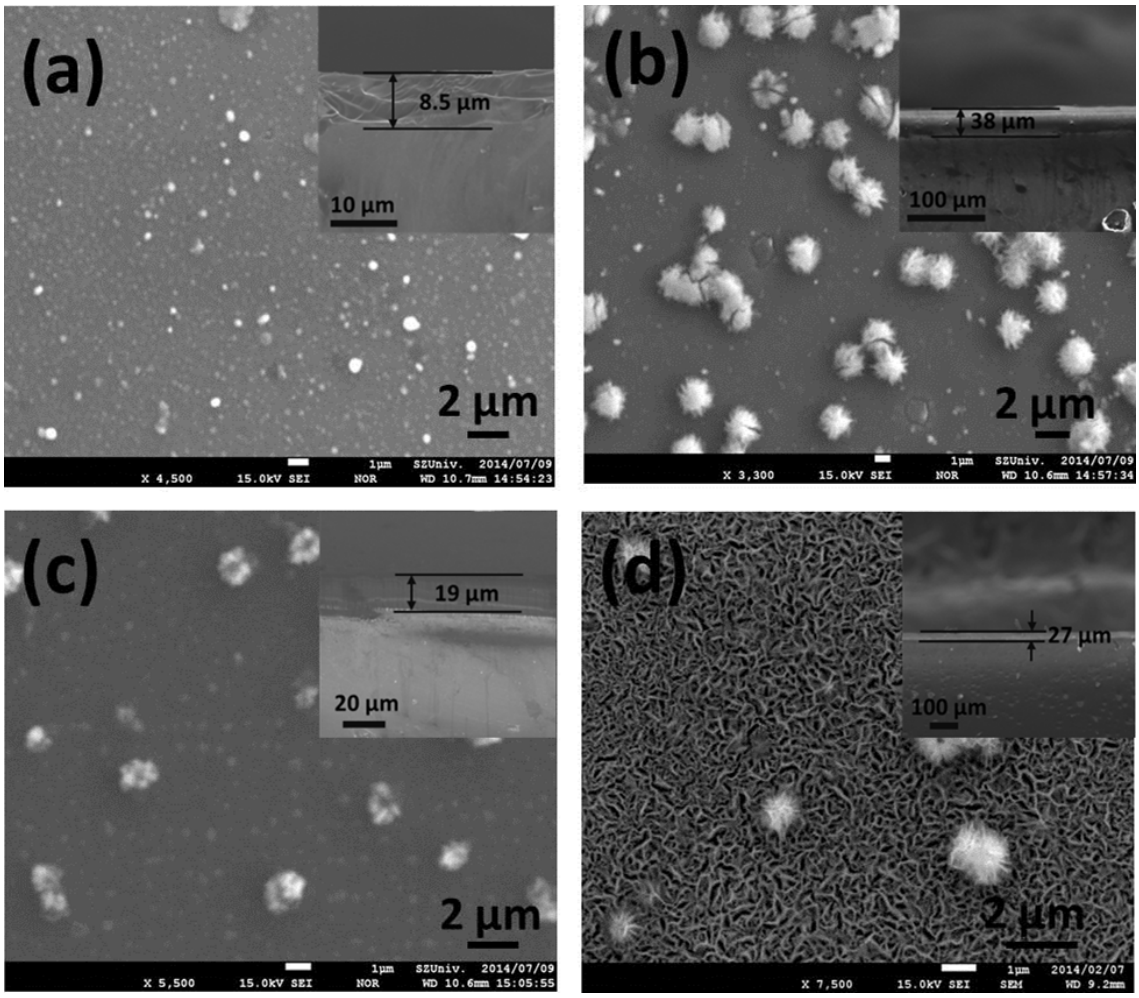

Fig. 3. SEM images of $Cu_{1-X}Cd_XS_2$ thin film samples A – D with cross-sectional images as inset, for thickness measurement

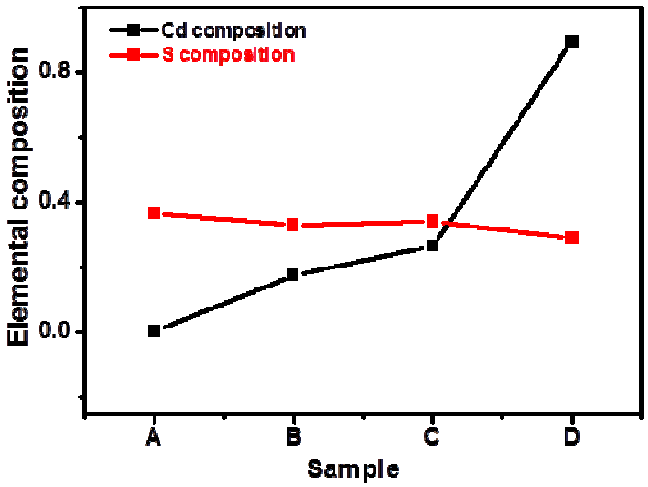

Fig. 4. Cd and S composition in deposited $Cu_{1-X}Cd_XS_2$ thin films measured by EPMA

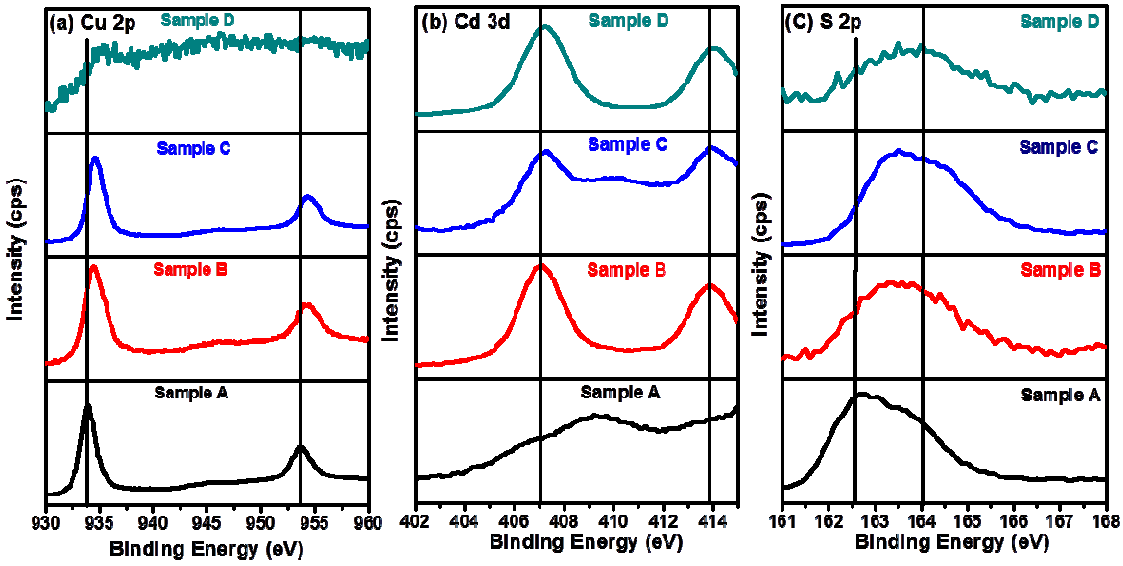

Fig. 5. XPS spectra of $Cu_{1-X}Cd_XS_2$ thin films showing binding energies of (a) Cu 2p (b) Cd 3d and (c) S 2p levels

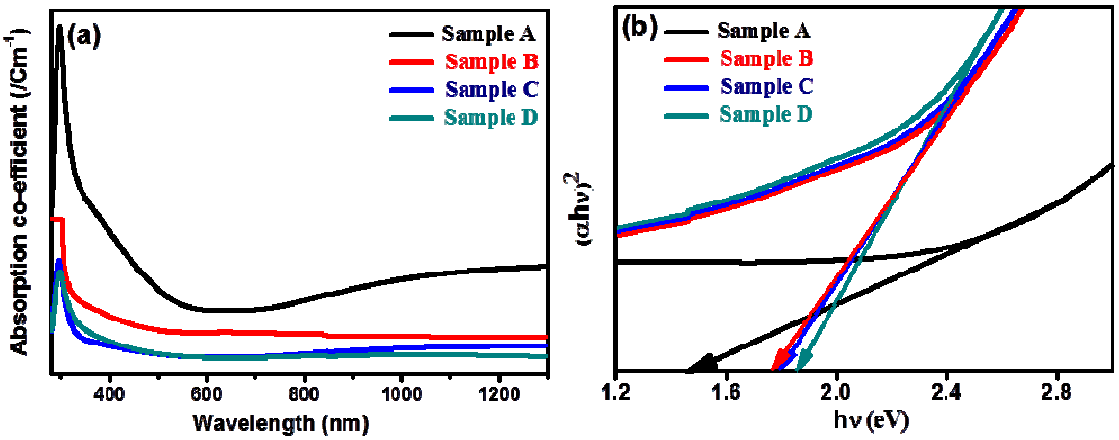

Fig. 6. (a) Absorption co-efficient Vs wavelength plot and (b) Tauc's plot of $Cu_{1-X}Cd_XS_2$ thin films

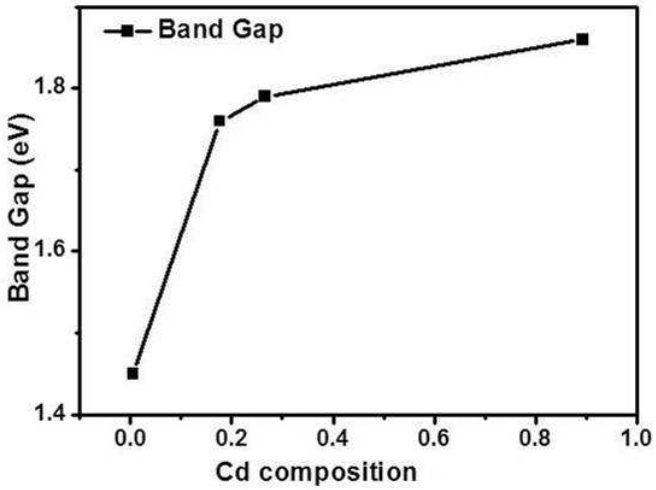

Fig. 7. Variation in band gap of $Cu_{1-X}Cd_XS_2$ thin films as a function of Cd composition

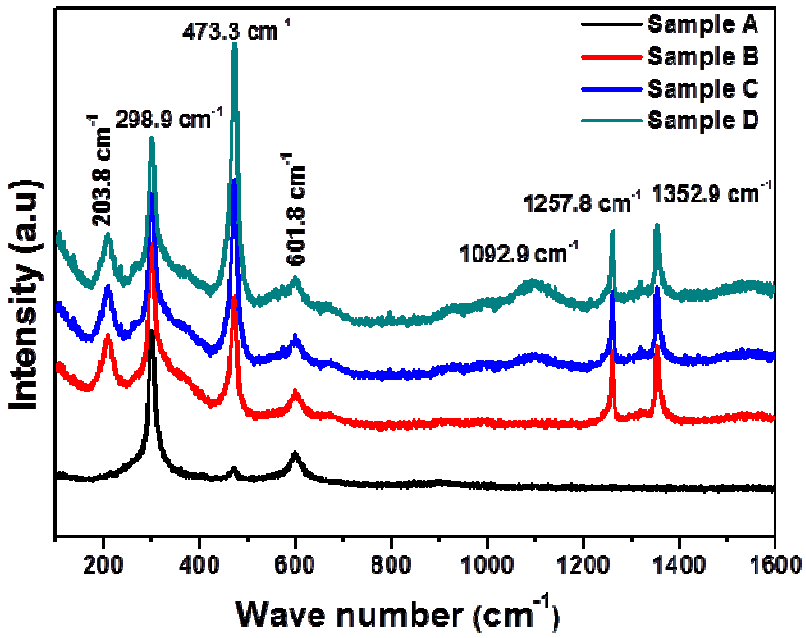

Fig. 8. Raman spectra of $Cu_{1-X}Cd_XS_2$ thin films